

Microstructural evolution in amorphous Al-based alloys

This article has been downloaded from IOPscience. Please scroll down to see the full text article.

2002 J. Phys.: Condens. Matter 14 L111

(<http://iopscience.iop.org/0953-8984/14/5/101>)

View [the table of contents for this issue](#), or go to the [journal homepage](#) for more

Download details:

IP Address: 171.66.16.27

The article was downloaded on 17/05/2010 at 06:05

Please note that [terms and conditions apply](#).

LETTER TO THE EDITOR

Microstructural evolution in amorphous Al-based alloys

Chuanjiang Zhang, Youshi Wu¹, Shouyi Dong, Yuanchang Shi,
Guorong Zhou and Chunxia Hu

College of Materials Science and Engineering, Shandong University (Southern Campus),
Jinan 250061, People's Republic of China

E-mail: zcjzxy@263.net (Youshi Wu)

Received 13 November 2001

Published 25 January 2002

Online at stacks.iop.org/JPhysCM/14/L111

Abstract

The $\text{Al}_{90}\text{Fe}_5\text{Ce}_5$ and $\text{Al}_{83}\text{Zn}_{10}\text{Ce}_7$ alloys were analysed with the aim of studying the microstructural evolution under various processing conditions. In addition to the icosahedral phase surrounded by the Al phase, the fine scale distribution of the metastable Al_6Fe phase produces on annealing the amorphous $\text{Al}_{90}\text{Fe}_5\text{Ce}_5$ alloy. In $\text{Al}_{83}\text{Zn}_{10}\text{Ce}_7$ alloy, the stable intermetallic compound Al_2ZnCe_2 forms as the primary phase during solidification. The precipitation nanocrystals of Al were accompanied with the intermetallic compound Al_2ZnCe_2 . For the amorphous Al-based alloys, the high glass formation appears to be controlled largely by the suppression of growth of nuclei formed during rapid melt quenching. The competitive nucleation and growth limitation of the various phases are attributed to the complex microstructures characteristic of the Al-based alloys.

Amorphous Al-based alloys containing rare earth (Re) and transition metals (TM) have good mechanical properties [1, 2]. Work on these materials has found that partially crystallized alloys, also termed nanocomposition, display outstanding mechanical strength [3,4]. Depending on chemical composition and quenching rate, a glassy, metastable crystalline phase or equilibrium intermetallic compound can be obtained.

The x-ray diffraction (XRD) patterns of many amorphous Al-based alloys show a pre-peak attributed to a strong chemical short-range order [5]. Recent research has shown a strong compound-forming tendency in favour of amorphous phase formation [6]. In general, the more chemical short-range order, the easier it is for the melt to crystallize. Complex phase selection behaviours have been reported in these alloys [7–9]. It is now evident that attention to the microstructural evolution of the amorphous Al-based alloys is essential in understanding glass stability, nanocrystallization reaction and in allowing for bulk glass synthesis.

¹ Author to whom any correspondence should be addressed.

This letter aims at the microstructural evolution in amorphous Al–TM–Re alloys. We select the Al–Fe system, the quasicrystals-forming system, as well as the Al–Zn system, a typical decomposition system, as our model system. This would help us better understand the complex microstructures characteristic of the Al-based alloys.

Alloy ingots were prepared by arc melting appropriate amounts of 99.99% Al, 99.99% Fe, 99.98% Zn and 99.9% Ce under argon atmosphere. Melt spinning was carried out in a partial helium atmosphere using a copper wheel. The ribbons were ~ 2 mm in width and ~ 25 μm in thickness. The structure of the ribbon samples was examined by XRD with monochromatic Cu K_{α} . Both isothermal and non-isothermal DSC experiments were carried out in a Netzsch DSC-404 system under a pure argon atmosphere. The selected temperature generally corresponds to the end of a thermal event. The microstructure changes in the amorphous $\text{Al}_{90}\text{Fe}_5\text{Ce}_5$ ribbons upon annealing were examined by transmission electron microscopy (TEM) techniques.

We have reported previously that a phase mixture (icosahedral surrounded by fcc-Al + amorphous) [10] can be obtained for $\text{Al}_{90}\text{Fe}_5\text{Ce}_5$ alloy by annealing the glass. We now reconsider the $\text{Al}_{90}\text{Fe}_5\text{Ce}_5$ alloy to provide a comparison with $\text{Al}_{83}\text{Zn}_{10}\text{Ce}_7$ alloy. Figure 1 shows the bright field micrographs and selected-area diffraction patterns of the amorphous $\text{Al}_{90}\text{Fe}_5\text{Ce}_5$ alloy annealed at 170°C for 30 min. The microstructure consisted of a homogenous distribution of nearly spherical particles embedded in the matrix. The distinct reflection rings taken from the near-spherical particles have been identified to be icosahedral (detailed studies in [10]). The ring pattern indicates that the icosahedral grains are very fine. The diffraction pattern corresponding to the icosahedral nanoparticles consists of distinct reflection rings with appreciable diffuseness, while the pattern corresponding to the fcc-Al phase consists of some reflection spots. It appears that the icosahedral nanoparticles are distributed in a surrounded state with a thin Al layer. In addition, there were regions with small plate-shaped particles parallel to each other that were identified as Al_6Fe (figures 1(a), (c)). Additional annealing at 170°C does not result in any significant coarsening of the icosahedral phase (figures 2(a)), while the crystals of Al_6Fe coarsen significantly and grow into the regions once occupied by the icosahedral phase (figures 2(b), (c)). It appears that the solid-state transformation of the amorphous to the icosahedral phase occurs homogeneously and the crystallization of Al suppresses the coarsening of icosahedral structure. But the presence of fcc-Al causes an increase in the formation rate of the metastable Al_6Fe phase. Whether the Al_6Fe is transformed from the icosahedral phase or grows from the matrix is unknown. It has been demonstrated that the icosahedral phase in Al–Fe–Ce alloy can be stable up to 800°C [11]. The present results suggest that Al_6Fe grows from the matrix. The conversion to Al_6Fe occurs along the amorphous inter-phase boundary eventually spreading into the interior of the amorphous phase.

The $\text{Al}_{83}\text{Zn}_{10}\text{Ce}_7$ ribbons always contain a fraction of crystal phases. An example is given in figure 3, where Al, Al_2ZnCe_2 and an amorphous phase are identified. These findings suggest that the formation of the Al_2ZnCe_2 phase is prone to nucleate from the melt and competes with the formation of the Al phase. By increasing the circumferential velocity of the copper wheel (up to 40 m s^{-1}), the amorphous single phase can be obtained for $\text{Al}_{83}\text{Zn}_{10}\text{Ce}_7$ alloy (figure 4(a)). In the XRD patterns taken after an isothermal anneal at 150°C for 5 min (figure 4(b)), the reflections of the Al_2ZnCe_2 phase appear in addition to the reflections of the Al phase. The same phases were found on the sample annealed at 150°C for 10 min with more intensity (figure 4(c)). It appears that the precipitation of Al accompanied the Al_2ZnCe_2 phase. Moreover, the presence of fcc-Al appears to favour the nucleation and growth of the Al_2ZnCe_2 phase.

High temperature analysis indicated that a primary intermetallic starts the equilibrium solidification [9]. DSC analysis revealed that Al precipitation from glassy matrices takes

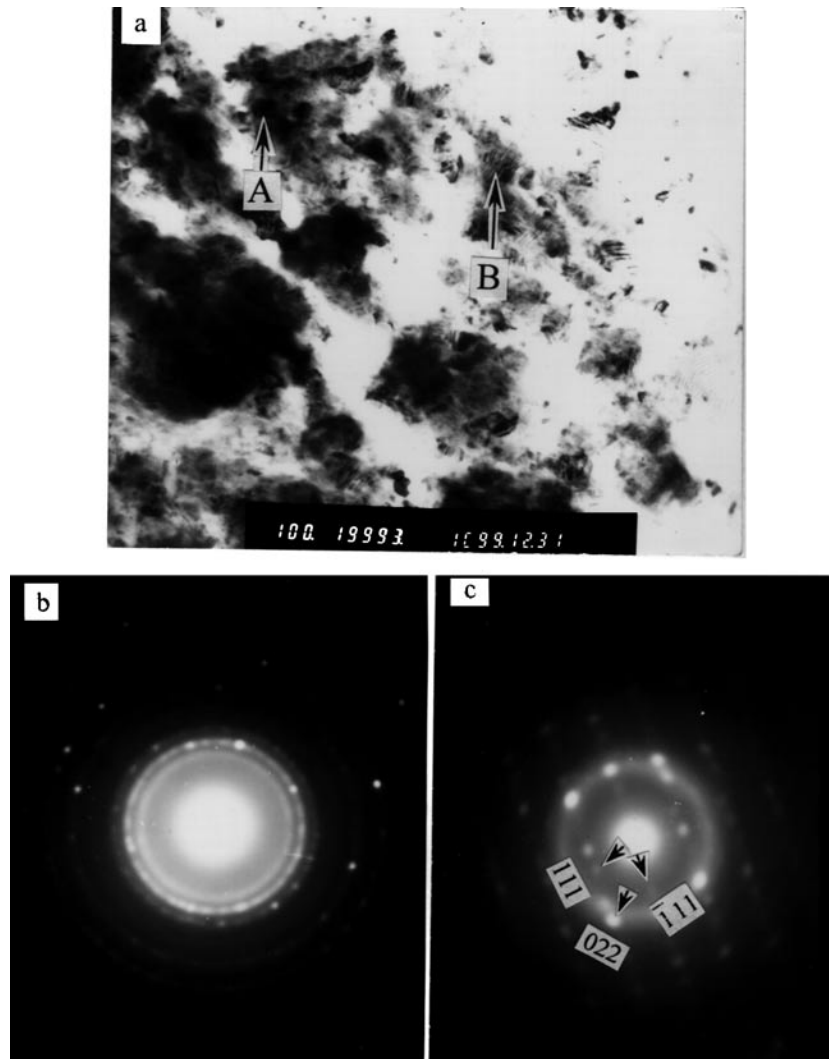


Figure 1. Transmission electron micrographs of the annealed $\text{Al}_{90}\text{Fe}_5\text{Ce}_5$ alloy: (a) bright-field image, A: near-spherical particles, B: small plate-shaped particles, (b) electron diffraction obtained from A, (c) electron diffraction obtained from B.

place at temperatures just above 150°C . Microstructures indicate that the icosahedral phase rejected excess Al as they were growing, causing Al to precipitate around the periphery of the icosahedral grain (figures 1(a), (b)). On the other hand, the presence of fcc-Al seems to favour the nucleation and growth of the crystalline phase. The notable examples are Al nanocrystals accompanied by the Al_2ZnCe_2 intermetallic in the $\text{Al}_{83}\text{Zn}_{10}\text{Ce}_7$ alloy and the Al_6Fe coupled with the Al phase in the $\text{Al}_{90}\text{Fe}_5\text{Ce}_5$ alloy. This could indicate that quench-in nuclei of intermetallics act as seeds for heterogeneous nucleation of Al in the glassy matrix. However, from our results, it appears that the competing Al_2ZnCe_2 phase nucleates with the Al phase in Al–Zn–Ce alloys and the competing metastable Al_6Fe phase nucleates with the icosahedral phase. The possibility of nucleating various phases may represent a ‘confusion principle’ for Al-based alloys helping in glass formation.

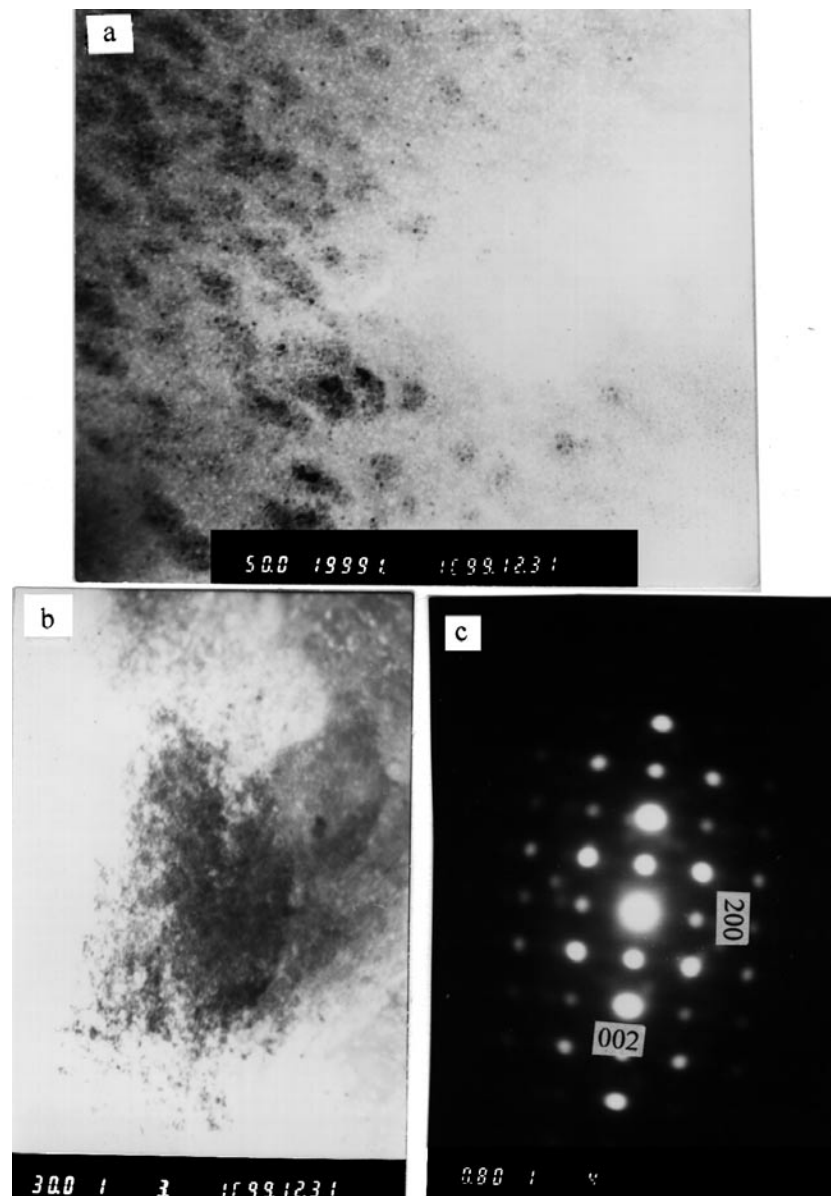


Figure 2. Transmission electron micrographs of the further annealed $\text{Al}_{90}\text{Fe}_5\text{Ce}_5$ alloy: (a) and (b) bright-field images, (c) electron diffraction obtained from (b).

The appearance of the pre-peak indicates the existence of a strong chemical short-range order [5]. Based on the shape and position of the peak of the structure factor, Murdryj *et al* [12] have pointed out that the chemical short-range order packed by unlike atoms could exist even in the melt of Al–Zn with high mutual solubility. The pre-peak has been observed in many Al-based alloys [6]. It has been demonstrated that the chemical short-range order in the Al-based metallic glasses is inherited from the melt [13]. Moreover, the existence of the chemical short-range order in the melt of Al-based alloys has been confirmed by x-ray scattering [13], neutron scattering [14] and EXAFS [15]. Quenching conditions have no

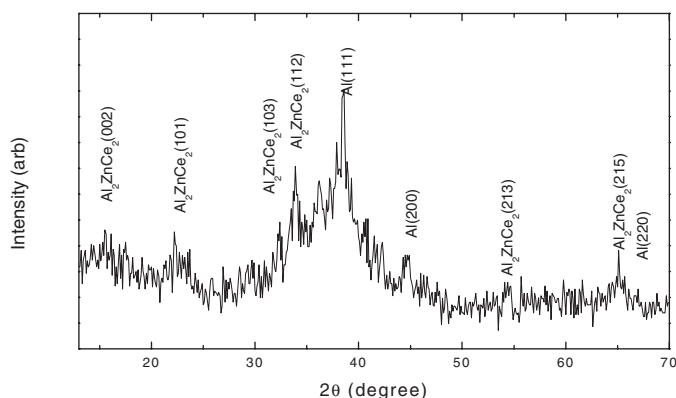


Figure 3. XRD patterns of the rapidly solidified $\text{Al}_3\text{Zn}_7\text{Ce}_{10}$.

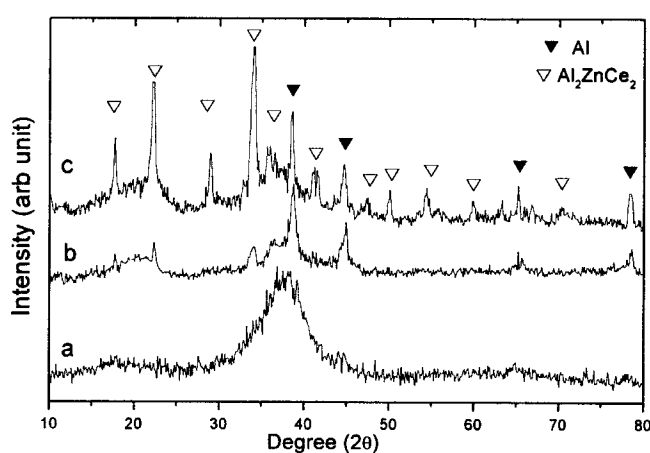


Figure 4. The XRD patterns of Al_2ZnCe_2 alloy: (a) as-rapidly solidified, (b) annealed at 150°C for 5 min, (c) annealed at 150°C for 10 min.

critical effects on the coordination of atoms in the short-range order of Al-based alloys [13]. The observation of pre-existed nuclei of fcc-Al plus icosahedral structure in the Al-Fe-Ce system and the fcc-Al plus intermetallic Al_2ZnCe_2 in the Al-Zn-Ce system further confirmed that nucleation could take place during the process of rapid solidification. These results indicate that in Al-TM-Re alloys glass formation is not controlled by nucleation restrictions. Based on the results of our experiments and others done before, the complex microstructures characteristic of the Al-based alloy are a strong function of the competitive nucleation and growth kinetics of various phases. The easy nucleation is due to the homogeneous existence of chemical short-range order in the melt. Microstructure analyses have shown that the icosahedral grains suppress the growth of fcc-Al as it is growing [10]. The kinetics of crystallization of Al-Mn alloy is a polymorphous transformation [16], while in Al-Ni-Ce alloy it is related to the long-range diffusion [17]. The present experimental results show that the primary compound Al_2ZnCe_2 simultaneously precipitates with the α -Al phase. Therefore, the competitive nucleation and growth restrictions are critical for the microstructure of the Al-based alloys.

In summary, we have studied the formation of the dispersoid in Al-based alloys. In addition to the icosahedral phase surrounded by the Al phase, the fine scale distribution of the metastable Al_6Fe phase produces on annealing the amorphous $\text{Al}_{90}\text{Fe}_5\text{Ce}_5$ alloy. In $\text{Al}_{83}\text{Zn}_{10}\text{Ce}_7$ alloy, the stable intermetallic compound Al_2ZnCe_2 forms as the primary phase during solidification. For the amorphous Al-based alloys, the high glass formation appears to be controlled largely by the suppression of growth of nuclei formed during rapid melt quenching. The competitive nucleation and growth limitation of the various phases are attributed to the complex microstructures characteristic of Al-based alloys. This study can give guidance in the control of amorphous phase stability and crystallization path for Al-based alloy.

This work was supported by the Natural Science Foundation of Shandong Province (project no Y2000B02).

References

- [1] He Y, Poon S J and Shiflet G J 1988 *Science* **241** 1640
- [2] Inoue A, Ohtera K, Zhang T and Masumoto T 1988 *Japan. J. Appl. Phys.* **27** L1583
- [3] Inoue A 1998 *Prog. Mater. Sci.* **43** 365
- [4] Gloriant T and Greer A L 1998 *Nanostruct. Mater.* **10** 389
- [5] Elliot S R 1991 *Phys. Rev. Lett.* **67** 711
- [6] Zhang L, Chen K, Huang X, Wu Y and Bian X 2001 *J. Phys.: Condens. Matter* **13** 5947
- [7] Herlach D M, Gillessen F, Volkmann T, Wollgarten M and Urban K 1992 *Phys. Rev. B* **46** 5203
- [8] Guo J Q and Ohtera K 1998 *Acta Mater.* **11** 3829
- [9] Rizzi P, Baricco M, Borace S and Battezzati L 2001 *Mater. Sci. Eng. A* **304–6** 574
- [10] Zhang C, Wu Y, Cai X, Zhou G, Shi Y, Yang H and Wu S 2001 *J. Phys.: Condens. Matter* **13** L647
- [11] Yang L Y, Zhao J G, Zhan W S, Yang C Y, Zhou Y Q and Fung K K 1987 *J. Phys. F: Met. Phys.* **17** L97
- [12] Murdryj S I, Galchak V P, Baskin V N and Skutor A K 1993 *Rasplavy* **3** 11
- [13] Zhang L, Wu Y, Bian X, Li H, Wang W, Li J and Lun N 1998 *J. Phys.: Condens. Matter* **11** 7959
- [14] Maret M, Pomme T, Pastarel A and Chieux P 1990 *Phys. Rev. B* **42** 1598
- [15] Jacobs G, Egry I, Holland-Moritz D and Platzek D 1998 *J. Non-Cryst. Solids* **232–4** 396
- [16] Chen L C, Spaepen F, Robertson J L, Moss S C and Hiraga K 1990 *J. Mater. Res.* **5** 1871
- [17] Tsai A P, Kaniyama T, Kawamura Y, Inoue A and Masumoto T 1997 *Acta Mater.* **45** 1477